Dalton Transactions

ROYAL SOCIETY OF CHEMISTRY

PAPER

View Article Online
View Journal | View Issue

Cite this: *Dalton Trans.*, 2025, **54**, 17196

Photochromic macrocyclic complexes of yttrium(III) undergoing merocyanine to spiropyran isomerization as models for single-molecule magnet switch candidates

Nour El Beyrouti,[a] Nadège Hamon,[b] Louis Caussin,[a] Yoann Fréroux,[a] Marie Dallon,[a] Thierry Roisnel,[a] Boris Le Guennic,[a] Stéphane Rigaut,[a] Raphaël Tripier[b] and Lucie Norel *[a,c]

The synthesis and characterization of four macrocyclic yttrium(III) or dysprosium(III) complexes bearing a merocyanine photochromic unit are reported. The diamagnetic yttrium(III) complexes allowed for NMR investigation of both the equilibrium state and the photoinduced species, and they were also characterized using single-crystal XRD. We conclude from these studies that merocyanine is the more stable isomer in all the investigated solvents (methanol, acetonitrile, and dichloromethane) and in the solid state. Detailed structural investigations of isomerization to spiropyran appear to be challenging in solution as well as in crystals. Theoretical studies calculated large energy differences between the merocyanine and spiropyran isomers, which depend on the substitution of the photochromic unit by nitro groups. They also reveal that such designs would be well suited to construct photoswitchable single-molecule magnets, since the anisotropy of the dysprosium(III) complexes is significantly affected by the isomeric state of the ligand.

Received 21st August 2025,
Accepted 15th October 2025

DOI: 10.1039/d5dt02008e

rsc.li/dalton

Introduction

Precisely designed lanthanide complexes can generate diverse magnetic behaviors with technological relevance depending on the choice of lanthanide ion and its coordination sphere.[1] Contrast agents based on macrocyclic gadolinium(III) complexes are part of our lives,[2] and single-molecule magnets based on the more anisotropic dysprosium(III) or terbium(III) ions have generated great expectations and have undergone extraordinary development in the last decade.[3] Indeed, the idea that the two magnetic states of these inherently bistable molecules could be used for nanoscale information storage is promoting this field of research. Using light as a remote control for the magnetic behavior of lanthanide complexes could lead to behaviors relevant to applications as light-activable contrast agents[4] or molecular magneto-optical memories.[5] Because lanthanide systems cannot be switched with light directly, the use of photochromic ligands to form the corresponding complexes is one attractive strategy in this context, which has already provided switchable contrast agents[6] and photomodulated single-molecule magnets.[7]

Louie *et al.* were the first to realize that spiropyran photoswitches are ideally suited for the manipulation of lanthanide complexes.[6,8] Indeed, the photogenerated isomer of spiropyran (SP), merocyanine (MC), exhibits a strongly coordinating phenolate oxygen that is not present in the SP isomer. Therefore, in the case of gadolinium(III) complexes having a macrocyclic ligand functionalized with such a unit,[6] it has naturally been hypothesized that the MC and SP isomers would provide different coordination environments, as depicted in Scheme 1. The accessibility of the metal to water,

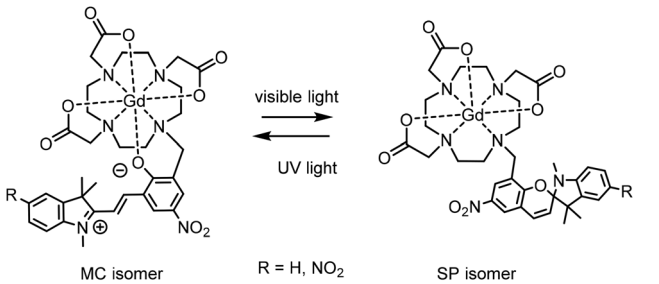

Scheme 1 Hypothesized isomerization in previously investigated gadolinium(III) complexes. See ref. 6.

[a]*Univ Rennes, INSA Rennes, CNRS, ISCR (Institut des Sciences Chimiques de Rennes) – UMR 6226, F-35000 Rennes, France. E-mail: lucie.norel@univ-rennes.fr*
[b]*Univ Brest, UMR-CNRS 6521 CEMCA, F 29200 Brest, France*
[c]*Institut Universitaire de France, France*

which directly affects the relaxivity, is different for each isomer. Our group soon realized that a similar process would be highly desirable to obtain photoswitchable single-molecule magnets, since the magnetic bistability of dysprosium(III) complexes is actually controlled by the axial character of the crystal field experienced by the metal to a great extent.[9] Hence, multidentate MC ligands are expected to generate an axial crystal field and strong magnetic anisotropy, in contrast to the SP isomer.[10]

On this basis, it can be envisioned that the dysprosium versions of two previously investigated gadolinium complexes[6] (Scheme 1) would allow investigation of how the photoinduced structural change impacts the magnetic behavior. However, this task is not trivial, because spiropyrans are T-type photochromes and therefore exist in an equilibrium between their two isomers that depends on many parameters such as concentration, solvent polarity or metal coordination.[11] We also previously demonstrated that the isomerization of the *trans*-MC form to the *cis*-MC state without the further formation of the SP isomer is an issue in related lanthanide complexes with non-macrocyclic ligands.[10] Additionally, complexity can arise from the many structural fluctuations of macrocyclic lanthanide(III) complexes in solution that result from the macrocycle conformation or solvent coordination.[12] Hence, it seemed important to remedy the lack of structural information on previously published gadolinium(III) complexes for both isomers by reinvestigating this system using appropriate Ln ions prior to investigation of the photomagnetic effects.

In this contribution, we report the synthesis and characterization of four new complexes of yttrium(III) and dysprosium (III) ions. The two investigated ligands differ by the presence of a nitro group on the indoline part of the photochromic unit, which has previously been shown to shift the equilibrium towards the SP isomer. The diamagnetic yttrium(III) complexes enabled NMR investigation of both the equilibrium state and the photoinduced species, and were also successfully characterized using XRD. We thus provide structural and spectroscopic evidence of the isomerization at play and its dependence on the presence of an electron-withdrawing group on the indoline moiety in various organic solvents.

Experimental

Complex 1Y

To a solution of $\mathbf{L_1}$ (32 mg, 47 μmol) in MeOH (10 mL) was added $YCl_3{\cdot}6H_2O$ (43 mg, 141 μmol, 3 equiv.). The reaction mixture was stirred at room temperature for 2.5 days before solvent evaporation to dryness. Purification of the crude by flash chromatography on C18-silica gel (Column C18-4g from Interchim, Eluent: H_2O/ACN 95/5 for 10 min, then H_2O/ACN 95/5 to 2/8 for 30 min, flow: 15 mL min^{-1}) gave **1Y** (31 mg, 40 μmol, y = 86%) as a dark orange amorphous solid. ESI-HR-MS (positive, MeOH) m/z calcd for $[C_{34}H_{42}N_6O_9Y]^+$: 767.2066, found: 767.2060, $[M + H]^+$; calcd for $[C_{34}H_{43}N_6O_9Y]^{2+}$: 384.1069, found: 384.1065, $[M + 2H]^{2+}$. ^{1}H NMR (500 MHz, CD_3OD): δ (ppm) = 8.63 (d, J = 3.0 Hz, 1H), 8.61 (bd, 1H, this signal tends to disappear upon standing in CD_3OD under 450 nm irradiation), 8.25 (d, J = 15.9 Hz, 1H, this signal transforms into a singlet upon standing in CD_3OD under 450 nm irradiation), 8.19 (d, J = 3.0 Hz, 1H), 7.76 (d, J = 7.1 Hz, 1H), 7.72 (d, J = 7.1 Hz, 1H), 7.60 (m, 2H), 4.27 (s, 3H), 3.8–2.2 (m, 24H), 1.83 (m, 6H). Electronic absorption (methanol): λ_{max1} = 352 nm (ε = 13 200 M^{-1} cm^{-1}), λ_{max2} = 468 nm (ε = 12 800 M^{-1} cm^{-1}).

Complex 1Dy

To a solution of $\mathbf{L_1}$ (59 mg, 87 μmol) in MeOH (10 mL) was added $DyCl_3{\cdot}6H_2O$ (49 mg, 130 μmol, 1.5 equiv.). The reaction mixture was stirred at room temperature for 4 days before solvent evaporation to dryness. Purification of the crude by flash chromatography on C18-silica gel (Column C18-4g from Interchim, Eluent: H_2O for 10 min, H_2O/ACN 100/0 to 0/100 for 30 min, 100% ACN for 10 min, flow: 10 mL min^{-1}) gave **1Dy** (49 mg, 58 μmol, y = 68%) as an orange amorphous solid. ESI-HR-MS (positive, MeOH) m/z calcd for $[C_{34}H_{43}DyN_6O_9]^+$: 421.6186, found: 421.6192, $[M + 2H]^{2+}$; calcd for $[C_{34}H_{42}DyN_6O_9]^+$: 842.2299, found: 842.2315, $[M + H]^+$. Electronic absorption (methanol): λ_{max1} = 352 nm (ε = 13 000 M^{-1} cm^{-1}), λ_{max2} = 468 nm (ε = 12 700 M^{-1} cm^{-1}).

Complex 2Y

A solution of $\mathbf{L_2}$ (202 mg, 278 μmol) and $YCl_3{\cdot}6H_2O$ (85 mg, 278 μmol) in 20 mL of methanol was refluxed for 18 h under argon. The solvent was evaporated to dryness. The residual solid was purified *via* silica column chromatography using dichloromethane/methanol/water (1 : 4 : 1) as the eluent to give **2Y** (149 mg, 183 μmol, y = 66%) as a red solid. ESI-HR-MS (positive, MeOH) m/z calcd for $[C_{34}H_{41}N_7O_{11}Y]^+$: 812.1917, found: 812.1918 $[M + H]^+$. ^{1}H NMR (400 MHz, CD_3OD): δ (ppm) = 8.6–8.7 (m, 3H), 8.49 (dd, J = 8.8, 2.2 Hz, 1H), 8.38 (d, J = 16.0 Hz, 1H), 8.20 (d, J = 3.1 Hz, 1H), 7.93 (d, J = 8.9 Hz, 1H), 4.7–2.1 (m, 24H), 4.28 (s, 3H), 1.90 (bs, 6H). Electronic absorption (methanol): λ_{max1} = 358 nm (ε = 13 000 M^{-1} cm^{-1}), λ_{max2} = 507 nm (ε = 12 800 M^{-1} cm^{-1}).

Complex 2Dy

A solution of $\mathbf{L_2}$ (170 mg, 234 μmol) and $DyCl_3{\cdot}6H_2O$ (88 mg, 234 μmol) in 20 mL of methanol was refluxed for 24 h under argon. The solvent was evaporated to dryness. The residual solid was purified *via* silica column chromatography using dichloromethane/methanol/water (1 : 4 : 1) as the eluent to afford complex **2Dy** (141 mg, 159 μmol, y = 68%) as a red solid. ESI-HR-MS (positive, MeOH) m/z calcd for $[C_{34}H_{43}DyN_6O_9]^+$: 421.6186, found: 421.6192, $[M + 2H]^{2+}$; calcd for $[C_{34}H_{41}DyN_7O_{11}]^+$: 887.2156, found: 887.2159, $[M + H]^+$. Electronic absorption (methanol): λ_{max1} = 358 nm (ε = 13 000 M^{-1} cm^{-1}), λ_{max2} = 507 nm (ε = 12 800 M^{-1} cm^{-1}).

Results and discussion

Synthesis and structure

The two spiropyran substituted DO3A proligands $\mathbf{L_1}$ and $\mathbf{L_2}$ (Scheme 2) were obtained according to published procedures[6a,c] with slight modifications and fully characterized (Fig. S1–S5). Subsequently, reaction with the appropriate metal salts provided the target complexes (Scheme 2) with moderate yields. Their purification was performed by flash chromatography on C18 grafted silica (**1M**) or silica (**2M**) gel. Details of the characterization can be found in SI (Fig. S6–S19). **1M** were found to be soluble in acetonitrile and methanol and sparingly soluble in dichloromethane, whereas for **2M**, the compounds were only sparingly soluble in methanol and water.

Complex **1Y** was crystallized by the aerial diffusion of ether into an acetonitrile solution, and complex **2Y** crystalized upon slow evaporation of a methanol solution. The resulting XRD data are described in the SI and can be accessed *via* CCDC deposition numbers 2346662 and 2346663. In brief, the *P*2/*c* space group was assigned to compound **1Y**, which crystalized with one acetonitrile molecule. The merocyanine isomer with the *trans* configuration of the double bond is clearly identified in this structure (Fig. 1 and S20). The merocyanine phenolate is involved in a coordination bond to the yttrium center, with a total coordination number of 8, since 3 oxygen and 4 nitrogen atoms from the DO3A moiety are also bound to Y. The DO3A moiety has a typical square antiprism geometry with the oxygen atom square being more "open" than the nitrogen one.[13] However, no additional solvent molecule is coordinated, probably because of the bulky merocyanine ligand. The yttrium phenolate bond has a length of 2.2552(17) Å and is the shortest among the coordination bonds (Table S2). This type

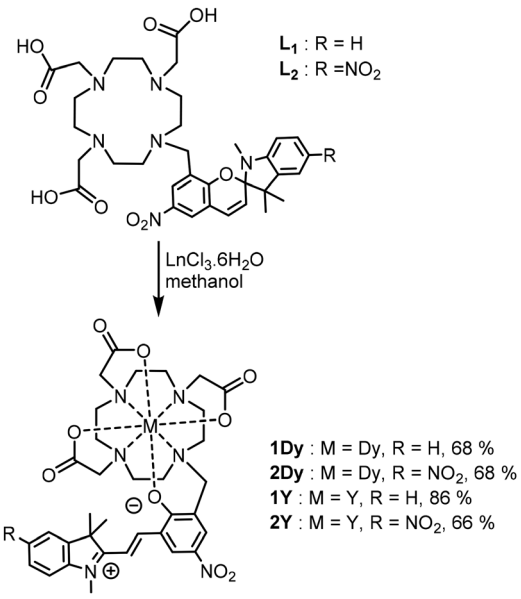

Scheme 2 Final step of the synthesis of **1M** and **2M**.

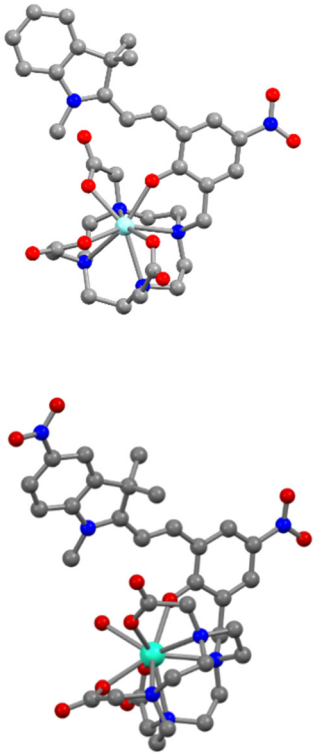

Fig. 1 View of the structure of **1Y** (top) and **2Dy-H_2O** (bottom) as determined from single-crystal X-ray diffraction data at 150 K. Grey, blue, red, light blue and light green spheres represent C, N, O, Y and Dy atoms, respectively. H atoms and solvent have been omitted for clarity.

of coordination environment is known to promote magnetic anisotropy in related DOTA complexes.[14] Compound **2Y** crystallizes in a triclinic $P\bar{1}$ space group and shows very similar features (Fig. S21, Tables S3 and S4).

The dysprosium complexes proved much more difficult to crystallize. We performed powder XRD on the obtained solids, but all samples were amorphous. However, in one isolated experiment that we were unable to reproduce, slow evaporation of a methanol/ethyl acetate solution of **2Dy** yielded a small amount of crystals with a very interesting structure (CCDC 2477727). Indeed, in this case, a *C*2/*c* space group was assigned to the structure, and a coordination number of 9 was found for the dysprosium center because of the incorporation of a water molecule in the coordination sphere (Fig. 1 and S22). To accommodate this change, all the Dy–O and Dy–N distances are longer (Table S4); for instance, the length of the dysprosium phenolate bond is 2.3252(19) Å, while it is 2.2477(18) in **2Y**. The structure of this compound, which was called **2Dy-H_2O**, indicates that the water accessibility for the merocyanine isomers is non-negligible; this indicates a need for caution in the interpretation of previous studies of macrocyclic spiropyran gadolinium complexes,[6] because the presented hypothesis regarding different solvation numbers of the two isomers to explain the relaxivity changes is in contradiction with the present structure.

To investigate photochromism at the single-crystal state, crystals of **1Y** were submitted to 450 nm irradiation, but

showed no change in color. We conclude that significant conversion to the SP isomer is not observed in the crystalline state. Furthermore, a KBr pellet of compound **1Y** showed the same absorption spectrum before and after irradiation with either 450 nm or white light (Fig. S42) indicating a lack of solid-state photochromism. This behavior is expected for such compounds, as the MC to SP conversion requires a crystal packing that provides sufficient free volume to accommodate the large molecular motion.[15]

Equilibrium composition

With the aim of efficiently crystallizing a single isomer, we became interested in the effect of solvent composition (methanol, acetonitrile, dichloromethane) on the equilibrium state of our four complexes. For the yttrium complexes, information from electronic absorption and NMR experiments can be easily combined to determine the composition. Indeed, the diamagnetic ^{1}H spectra of SP and MC isomers are very distinctive, with the ethylenic protons showing either *cis* or *trans* coupling and the N–CH_3 signal being strongly deshielded in the MC isomer compared to the SP isomer. SP isomers also display weak absorption in the visible range, while the MC complexes typically show a broad absorption centred around 450–550 nm. In d^4-methanol, **2Y** showed doublets at 8.63 ppm and 8.38 ppm with J = 16.0 Hz and one singlet at 4.28 ppm, which were assigned to the double bond and N–CH_3 protons of the *trans*-merocyanine isomer, respectively. This was confirmed by the strong absorption band at 507 nm in methanol solution (Fig. 2, top). Under the same conditions, **1Y** showed doublets at 8.61 ppm and 8.25 ppm with J = 15.9 Hz, one singlet at 4.27 ppm and a strong absorption band at 468 nm (Fig. 2, top).

Therefore, both yttrium complexes show the same behaviour in methanol; the only appreciable difference is, as expected, the bathochromic shift of the merocyanine band when a nitro group is present on the indoline side, which destabilizes the MC ground state. Comparison with the absorption spectra of the dysprosium complexes clearly shows that the equilibrium composition is also shifted towards the merocyanine isomer in methanol for **1Dy** and **2Dy** (Fig. 2, top).

In d^3-acetonitrile and d^2-dichloromethane, the MC isomer was also the only one observed for **1Y**, and the electronic absorption data (Fig. 2) confirm that for **1Y** and **1Dy**, the MC isomer was the major one in the three solvents used (methanol, acetonitrile, dichloromethane). For **2Y** and **2Dy**, the MC isomer is also the major isomer in dichloromethane, whereas in acetonitrile, the MC band is slightly less intense relative to the higher energy transitions (Fig. 2, bottom), a fact that we assign to a moderate shift of the equilibrium towards the SP isomer in this specific solvent. Unfortunately, **2Y** is not soluble enough in these solvents for analysis of the equilibrium composition *via* NMR.

Altogether, we have provided conclusive evidence that in the solid state and in three organic solvents, the complexes exist mainly or exclusively as MC isomers, as supposed by Louie *et al.* for the gadolinium(III) analogues in water.[6]

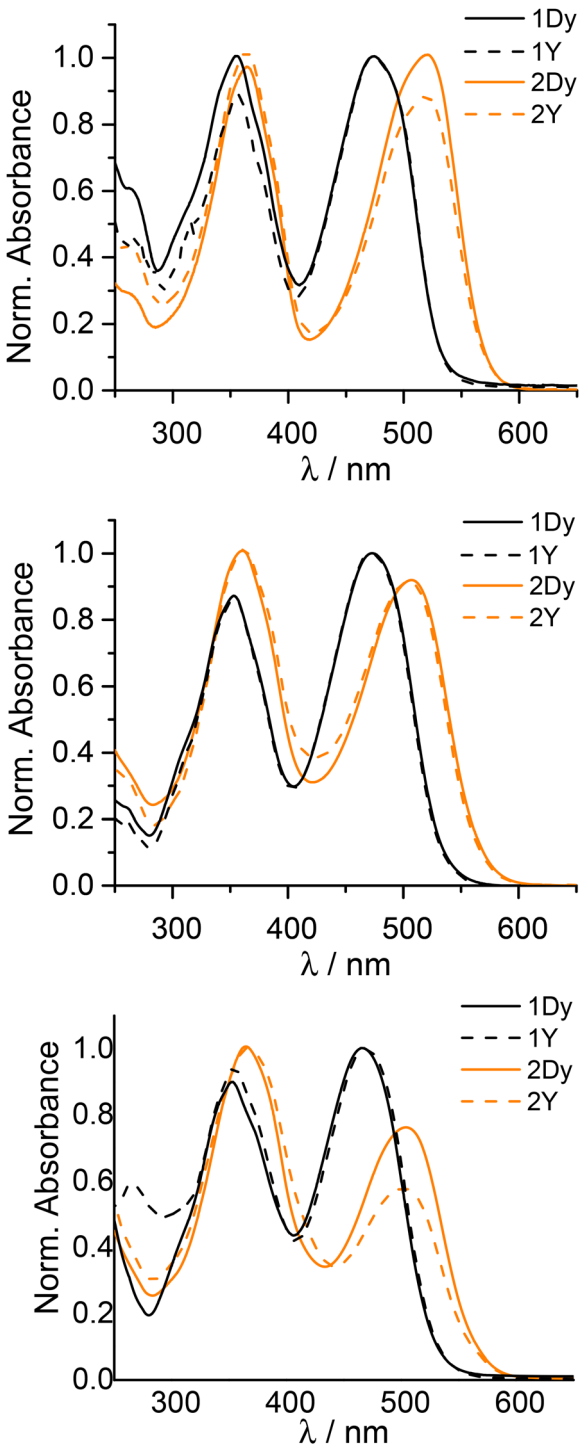

Fig. 2 Normalized electronic absorption spectra of the four complexes in methanol (top), dichloromethane (middle), and acetonitrile (bottom). The value of c ranged from 1 to 6 × 10^{-5} M depending on the sample.

Photochromism (NMR and electronic absorption studies)

Upon light irradiation, the initial orange (red) colour of complexes **1M** (**2M**) fades and is replaced with a light-yellow colour. We thus investigated the photochromic behaviour of the four complexes in all the previously studied solvents. In all

cases, **1Y** and **1Dy** showed similar behaviour, as did **2Y** and **2Dy**. Therefore, we discuss only the behaviour of **1Y** and **2Y** here (Fig. 3), while the corresponding dysprosium(III) complexes are described in the SI. For **1Y**, the most spectacular change in the absorption spectra was seen when dichloromethane was used as the solvent (Fig. 3a). After irradiation with 450 nm light for 3 min, the visible absorption vanished almost completely and a new transition at 270 nm appeared. The changes were reversible upon leaving the solution to stand in the dark for 3 days. A similar outcome was produced by the irradiation of an acetonitrile solution of **1Y**, but longer irradiation times (38 min) were necessary to reach the photostationary state (Fig. 3c). We also noticed that the rate of back-isomerization is faster in this solvent, since only 1 hour was necessary for reversion to the initial equilibrium state and corresponding spectrum. Finally, in methanol, irradiation with 450 nm light led to a photostationary state that still showed significant absorption at 468 nm, and a fast return to the equilibrium state was also observed (Fig. 3b). This fast return has a first-order kinetic constant of 0.17 h^{-1} at 20 °C (Fig. S25). These changes could be explained by the formation of the spiropyran isomer upon blue light irradiation (with an isomerization quantum yield of 0.6 ± 0.1), which spontaneously reverts to the most stable merocyanine isomer. In the case of **2Y**, irradiation was performed at 530 nm and similar changes in the absorption spectra were witnessed, but with a total lack of thermal reversibility in the dichloromethane and acetonitrile solutions (Fig. 3d and f). Only methanol solutions of **2Y** showed a reversible change upon 530 nm irradiation, and similarly to **1Y**, long irradiation times were needed and fast reversion to the initial state occurred (Fig. 3e). The isomerization quantum yield was 0.5 ± 0.1 and the value of the return first-order kinetic constant was 1.8×10^{-2} h^{-1} at 20 °C for **2Dy** (Fig. S26).

To identify the nature of the photoinduced species, we subjected NMR samples to blue light exposure (Fig. 4). For **1Y** in d^2-dichloromethane, after 3 h of irradiation at 450 nm, the sample turned pale yellow, and the NMR spectrum was drastically modified and somewhat broadened. It was clear that the initial MC isomer was transformed; for instance, the N–CH_3 signal at 4.38 ppm and the –$C(CH_3)_2$ one at 1.82 ppm lost most of their initial intensity, and new broad signals were observed at 1.2 ppm and 2.8 ppm and between 6 and 7 ppm. Upon returning to the equilibrium state, the MC isomer signals were again observed, and the signals for the remaining metastable photoinduced species became narrower, such that we observed, for instance, a doublet at 5.94 ppm (J = 10.4 Hz). The two possible structures after irradiation are: (1) the spiropyran isomer, which usually shows two inequivalent methyl groups at 1–1.3 ppm, the N–CH_3 signal at around 3 ppm and one alkene proton as low as 5.8–6 ppm with a J coupling of around 10 Hz,[16] and (2) the *cis* isomer of the MC, which we

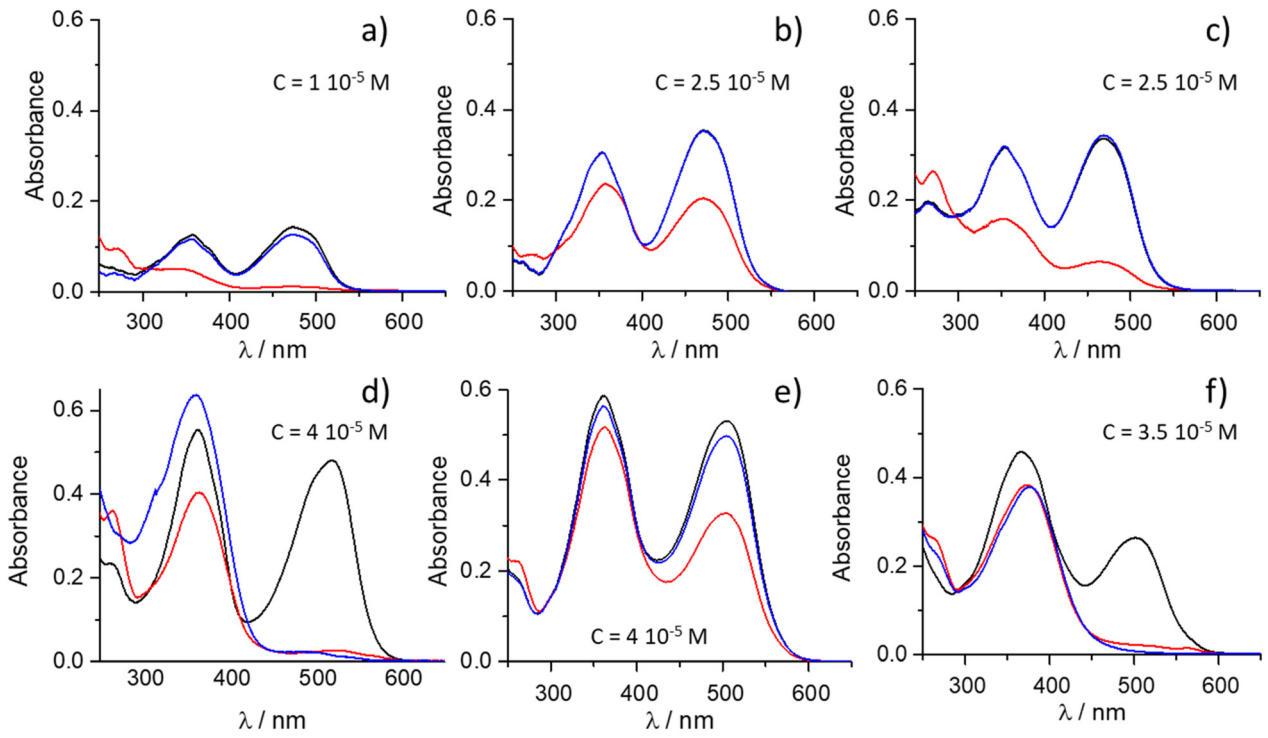

Fig. 3 Electronic absorption spectra of complex **1Y** (top) and **2Y** (bottom) in dichloromethane (left), methanol (middle) or acetonitrile (right) in the equilibrium state (black line), after irradiation (red line) and after being allowed to stand in the dark (blue line). Irradiation was performed at 450 nm (0.5 mW cm^{-2}) for **1Y** and at 530 nm (0.3 mW cm^{-2}) for **2Y**. Irradiation and resting times are as follows: (a) 450 nm – 3 min, dark – 72 h; (b) 450 nm – 10 min, dark – 2 h; (c) 450 nm – 38 min, dark – 1 h; (d) 530 nm – 7 min, dark – 12 h; (e) 530 nm – 75 min, dark – 1 h; and (f) 530 nm – 3 min, dark – 24 h. T = 20 °C.

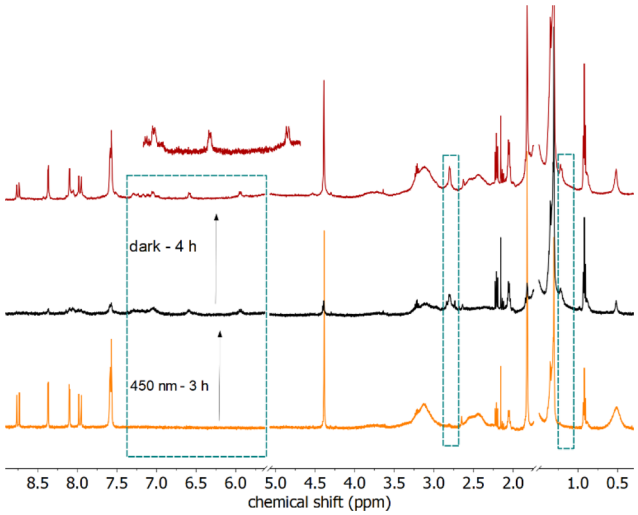

Fig. 4 ^{1}H NMR spectra (d^{2}-dichloromethane) of compound **1Y** at equilibrium (orange), after 3 h under 450 nm irradiation (black, 0.5 mW cm^{-2}), and after being allowed to stand in the dark for 4 h (red). The initial spectrum was recovered after two days in the dark.

previously identified in a similar structure by two equivalent methyl groups at 1.7 ppm, the N–CH_3 signal at 3.3 ppm and the alkene protons at 6.5 ppm with $J \approx 12$ Hz.[10a] Our observations are therefore indicative of a spiropyran isomer. The broad features could be explained as resulting from a mixture of different conformers with SP arms, which evolves toward a better-defined species with time. Unfortunately, the investigations in other solvents (d^{3}-acetonitrile and d^{4}-methanol, Fig. S40 and S41) yielded similar results, and low temperature NMR data were also inconclusive because of the precipitation of **1Y** or **2Y** at low temperatures. Note that H/D exchange of one of the alkene protons was observed during the course of this study when using d^{4}-methanol, in line with a previous report (Fig. S40).[16] For **2Y**, for solubility reasons, only d^{4}-methanol could be used as a solvent, but its fast return to equilibrium in this solvent made it very difficult to observe any photogenerated species. Therefore, we could not further explain the lack of reversibility in the case of **2Y** (and **2Dy**). For **1Y** (and **1Dy**), our findings support the initially assumed isomerization process (Scheme 1) but indicate that the photogenerated species is probably undergoing dynamic equilibrium between closely related SP structures, rendering its definitive structural characterisation difficult.

Theoretical calculations

As the experimental characterization of the photogenerated species in solution was challenging, we performed complementary theoretical calculations with several goals in mind: (i) to obtain the structure of the most stable isomer in different solvents, (ii) to determine the energy difference of the metastable state (SP isomer) and (iii) to assess the potential of such complexes for SMM switching.[3e] DFT geometry optimizations were performed on the four complexes **1M** and **2M** (M = Y, Dy) starting from the single crystal XRD structure obtained for **1Y** and taking the solvent into account using a polarizable continuum model (for dichloromethane and methanol). A spiropyran isomer was then constructed and optimized in order to evaluate the energy difference associated with the isomerization process. For all four complexes, the merocyanine isomer was found to be the most stable, in accordance with our experimental observations. In the case of **2Y** and **2Dy**, the spiropyran isomer was found to be 17–19 kcal mol^{-1} higher in energy (in the gas phase or with PCM dichloromethane or methanol, Table S6), whereas in the case of **1Y** and **1Dy**, the converged spiropyran forms are significantly higher in energy (20–25 kcal mol^{-1}). Moreover, it should be noted that in these latter cases only, several attempts (with various starting geometries) were necessary to stabilize the spiropyran forms, as the geometry optimizations had the tendency to converge as a merocyanine isomer. This is in line with the additional nitro group in **2M** being necessary to stabilize the spiropyran isomer. As a perspective for future manipulation of magnetic properties through photoswitching in this family of complexes, CASSCF/RASSI-SO calculations were carried out on the gas-phase optimized structures of the spiropyran and merocyanine forms of **1Dy** (see Computational details). The computed energy and wavefunction composition for each M_J state of the ground-state multiplet, as well as the component values of the Lande g factor are given in Tables S7 and S8. Significant differences are observed between isomers with the merocyanine form, which presents a ground state with an almost pure $|\pm 15/2\rangle$ contribution giving rise to an Ising g-tensor ($g_x = g_y = 0$; $g_z = 19.8$), a prerequisite for observing significant SMM behavior. The orientation of the corresponding easy axis is represented in Fig. S44. On the contrary, the spiropyran form presents less Ising ground state with a first excited state closer in energy. This difference in SMM behaviour is well illustrated computationally by the calculated magnetic transition moments (Fig. S43). These calculations thus confirm our hypothesis concerning the possibility of using light-induced isomerization of the MC arm to switch the SMM behavior of complex **1Dy** on and off. Unfortunately, the persistent difficulties in obtaining single crystals or microcrystalline samples for this compound preclude any meaningful magnetic investigation at this stage.

Conclusions

In this work, we have provided structural evidence relating to the photoisomerization of four macrocyclic complexes bearing a merocyanine photochrome. It was found that the equilibrium state of these complexes is dominated by the merocyanine isomer. The clear influence of substitution with a nitro group on the indoline moiety was evidenced both experimentally and theoretically by complexes **2Y** and **2Dy**, as the spiropyran isomer was stabilized by more than 7 kcal mol^{-1}. However, these complexes also showed less-reversible MC → SP photochromic behaviour in solution and a lack of solubility. For complex **1Y**, NMR investigation combined with geometry

optimization indicated the formation of a spiropyran isomer upon irradiation with 450 nm light. In addition, theoretical evaluation of the magnetic properties of each isomer of complex **1Dy** indicated significant variations in the axial character and the splitting energy between Kramers doublets when comparing the merocyanine and spiropyran isomers. Unfortunately, experimental confirmation could not be obtained because of the difficulty of preparing structurally characterized samples in the case of dysprosium. Nevertheless, these results highlight the strong potential of photochromic macrocyclic complexes for the development of photoswitchable single-molecule magnets.

Author contributions

Conceptualization: R. T., S. R. and L. N. Investigation: N. E. B., N. H., L. C., Y. F., T. R., M. D., B. L. G. Supervision: R. T., L. N. Visualization: L. N., N. E. B. Writing draft: N. H., N. E. B., L. N. Reviewing and editing: all authors.

Conflicts of interest

There are no conflicts to declare.

Data availability

The data supporting this article have been included as part of the supplementary information (SI). Supplementary information: ligand synthesis, NMR spectra, crystallographic studies, and details about electronic absorption and photochromism. See DOI: https://doi.org/10.1039/d5dt02008e.

CCDC 2346662, 2346663 and 2477727 (**1Y**, **2Y** and **2Dy·H_2O**) contain the supplementary crystallographic data for this paper.[17a–c]

Acknowledgements

We thank Pramila Selvanathan for preliminary synthesis tests. This project received funding from the Agence Nationale de la Recherche (ANR-18-CE07-0041-01). BLG thanks the French GENCI/IDRIS-CINES centers for high-performance computing resources.

References

1 A. Raza and M. Perfetti, *Coord. Chem. Rev.*, 2023, **490**, 215213.
2 T. J. Clough, L. Jiang, K.-L. Wong and N. J. Long, *Nat. Commun.*, 2019, **10**, 1420.
3 (*a*) J. D. Rinehart and J. R. Long, *Chem. Sci.*, 2011, **2**, 2078–2085; (*b*) R. Sessoli and A. K. Powell, *Coord. Chem. Rev.*, 2009, **253**, 2328–2341; (*c*) D. N. Woodruff, R. E. P. Winpenny and R. A. Layfield, *Chem. Rev.*, 2013, **113**, 5110–5148; (*d*) S. T. Liddle and J. van Slageren, *Chem. Soc. Rev.*, 2015, **44**, 6655–6669; (*e*) J.-L. Liu, Y.-C. Chen and M.-L. Tong, *Chem. Soc. Rev.*, 2018, **47**, 2431–2453; (*f*) O. Cador, B. Le Guennic and F. Pointillart, *Inorg. Chem. Front.*, 2019, **6**, 3398–3417; (*g*) C. A. P. Goodwin, F. Ortu, D. Reta, N. F. Chilton and D. P. Mills, *Nature*, 2017, **548**, 439–442; (*h*) F.-S. Guo, B. M. Day, Y.-C. Chen, M.-L. Tong, A. Mansikkamäki and R. A. Layfield, *Science*, 2018, **362**, 1400.
4 M. Dommaschk, J. Gröbner, V. Wellm, J.-B. Hövener, C. Riedel and R. Herges, *Phys. Chem. Chem. Phys.*, 2019, **21**, 24296–24299.
5 X. W. Feng, C. Mathoniere, I. R. Jeon, M. Rouzieres, A. Ozarowski, M. L. Aubrey, M. I. Gonzalez, R. Clerac and J. R. Long, *J. Am. Chem. Soc.*, 2013, **135**, 15880–15884.
6 (*a*) C. Tu and A. Y. Louie, *Chem. Commun.*, 2007, 1331–1333; (*b*) C. Tu, R. Nagao and A. Y. Louie, *Angew. Chem., Int. Ed.*, 2009, **48**, 6547–6551; (*c*) C. Tu, E. A. Osborne and A. Y. Louie, *Tetrahedron*, 2009, **65**, 1241–1246.
7 (*a*) M. Hojorat, H. Al Sabea, L. Norel, K. Bernot, T. Roisnel, F. Gendron, B. Le Guennic, E. Trzop, E. Collet, J. R. Long and S. Rigaut, *J. Am. Chem. Soc.*, 2020, **142**, 931–936; (*b*) G. Cosquer, B. K. Breedlove and M. Yamashita, *Dalton Trans.*, 2015, **44**, 2936–2942; (*c*) Z. Zhu, X.-L. Li, S. Liu and J. Tang, *Inorg. Chem. Front.*, 2020, **7**, 3315–3326.
8 (*a*) M. Gao, B. Shen, J. Zhou, R. Kapre, A. Y. Louie and J. T. Shaw, *ACS Omega*, 2020, **24**, 14759–14766; (*b*) B. Shen, M. Gao, F. C. Franco, R. Kapre, J. Zhou, X. Li, J. Garcia, J. T. Shaw and A. Y. Louie, *J. Org. Chem.*, 2020, **85**, 7333–7341.
9 K. L. M. Harriman, D. Errulat and M. Murugesu, *Trends Chem.*, 2019, **1**, 425–439.
10 (*a*) P. Selvanathan, V. Dorcet, T. Roisnel, K. Bernot, G. Huang, B. Le Guennic, L. Norel and S. Rigaut, *Dalton Trans.*, 2018, **47**, 4139–4148; (*b*) P. Selvanathan, G. Huang, T. Guizouarn, T. Roisnel, G. Fernandez-Garcia, F. Totti, B. Le Guennic, G. Calvez, K. Bernot, L. Norel and S. Rigaut, *Chem. – Eur. J.*, 2016, **22**, 15222–15226.
11 (*a*) R. Klajn, *Chem. Soc. Rev.*, 2014, **43**, 148–184; (*b*) L. Kortekaas and W. R. Browne, *Chem. Soc. Rev.*, 2019, **48**, 3406–3424.
12 L. G. Nielsen and T. J. Sørensen, *Inorg. Chem.*, 2020, **59**, 94–105.
13 G. Cucinotta, M. Perfetti, J. Luzon, M. Etienne, P.-E. Car, A. Caneschi, G. Calvez, K. Bernot and R. Sessoli, *Angew. Chem., Int. Ed.*, 2012, **51**, 1606–1610.
14 M.-E. Boulon, G. Cucinotta, J. Luzon, C. Degl'Innocenti, M. Perfetti, K. Bernot, G. Calvez, A. Caneschi and R. Sessoli, *Angew. Chem., Int. Ed.*, 2013, **52**, 350–354.
15 D. G. Patel, J. B. Benedict, R. A. Kopelman and N. L. Frank, *Chem. Commun.*, 2005, 2208–2210.
16 J. Garcia, J. B. Addison, S. Z. Liu, S. Lu, A. L. Faulkner, B. M. Hodur, E. I. Balmond, V. W. Or, J. H. Yun, K. Trevino, B. Shen, J. T. Shaw, N. L. Frank and A. Y. Louie, *J. Phys. Chem. B*, 2019, **123**, 6799–6809.

17 (*a*) CCDC 2346662: Experimental Crystal Structure Determination, 2025, DOI: 10.5517/ccdc.csd.cc2jrwsz; (*b*) CCDC 2346663: Experimental Crystal Structure Determination, 2025, DOI: 10.5517/ccdc.csd.cc2jrwt0; (*c*) CCDC 2477727: Experimental Crystal Structure Determination, 2025, DOI: 10.5517/ccdc.csd.cc2p58pv.